J Neurophysiol 104: 160–168, 2010.
First published March 24, 2010; doi:10.1152/jn.00029.2009.

Carving the Clock at Its Component Joints: Neural Bases for Interval Timing

Elaine B. Wencil,[1,3,4] H. Branch Coslett,[2-4] Geoffrey K. Aguirre,[2-4] and Anjan Chatterjee[2-4]
[1]*Departments of Psychology and* [2]*Neurology and* [3]*Centers for Cognitive Neuroscience and* [4]*Functional Neuroimaging, University of Pennsylvania, Philadelphia, Pennsylvania*

Submitted 9 January 2009; accepted in final form 19 March 2010

Wencil EB, Coslett HB, Aguirre GK, Chatterjee A. Carving the clock at its component joints: neural bases for interval timing. *J Neurophysiol* 104: 160–168, 2010. First published March 24, 2010; doi:10.1152/jn.00029.2009. Models of time perception often describe an "internal clock" that involves at least two components: an accumulator and a comparator. We used functional magnetic resonance imaging to test the hypothesis that distinct distributed neural networks mediate these components of time perception. Subjects performed a temporal discrimination task that began with a visual stimulus (S1) that varied parametrically in duration of presentation. A varying interstimulus interval was followed by a second visual stimulus (S2). After the S2 offset, the subject indicated whether S2 was longer or shorter than S1. We reasoned that neural activity that correlated with S1 duration would represent accumulator networks. We also reasoned that neural activity that correlated with the difficulty of comparisons for each paired-judgment would represent comparator networks. Using anatomically defined regions of interest, we found duration of S1 significantly correlated with left inferior frontal, supplementary motor area (SMA) and superior temporal regions. Furthermore, task difficulty correlated with activity within bilateral inferior frontal gyri. Therefore accumulator and comparator functioning of the internal clock are mediated by distinct as well as partially overlapping neural regions.

INTRODUCTION

Timing is essential to all behavior. Without the ability to accurately represent time ranging from hundreds of milliseconds to minutes, processes such as associative learning, sequencing, preparation, and planning would be difficult, and the everyday abilities that these processes support would be impossible. However, compared with spatial perception, relative little is known about the neural substrate of temporal perception. In the current study, we used functional magnetic resonance imaging (fMRI) to identify the anatomical correlates of putative components of an internal clock that underly interval timing.

Functional imaging studies of interval timing have not been consistent in their reports of neural activation patterns (reviewed in Harrington and Haaland 1999; Lewis and Miall 2003; Macar et al. 2002; Meck et al. 2008). These inconsistencies might arise from differences in experimental design and analyses. Studies have used a variety of tasks, including finger tapping (Lang et al. 1990), temporal discrimination (Casini and Macar 1996; Coull et al. 2004; Rao et al. 2001), time production (Macar et al. 2004; Tracy et al. 2000), and time reproduction (Casini and Macar 1996). These experimental designs differ with respect to motor planning, attention, cognitive load, and memory demands, any or all of which might contribute to differences in neural activity. In addition, the sensory modality of the stimuli to be timed varies across studies. Some studies use visual (Coull et al. 2004; Pouthas et al. 2000; Rubia et al. 1998), others auditory (Brunia et al. 2000; Rao et al. 1997, 2001), tactile (Macar et al. 2004), or no sensory stimulus at all (Lang et al. 1990; Tracy et al. 2000). The significance of experimental variables was reinforced when two conflicting, previously published neuroimaging datasets were re-analyzed taking different task demands into account (Lewis and Miall 2006a). By accounting for differing designs and standardizing analysis steps, they found comparable timing related activation across both tasks. Right posterior parietal activation was related to attentional processes, whereas right dorsolateral prefrontal cortex related to working memory. Another difference is the way component processes are operationalized. For example, one study interpreted bilateral cerebellar and right dorsolateral prefrontal cortex activation 7.5 s after the duration onset in a temporal discrimination task as representative of comparator functions (Rao et al. 2001). By contrast, when comparing easy versus hard trials in a similar task, left middle-frontal, bilateral parietal, left inferior-frontal, and superior temporal cortex activations were attributed to comparator functions (Harrington et al. 2004).

Designing fMRI studies to assess temporal representation presents particular challenges (Meck and Malapani 2004). One important consideration is choosing an appropriate baseline or control task. Studies contrasting time discriminations to intensity discriminations (e.g., which tone is louder?) (Macar et al. 1999; Pouthas et al. 2000) or to cued responses (Kawashima et al. 2000; Lejeune et al. 1997) can produce two confounds. *1*) Temporal decisions occur over the course of the trial, whereas these control tasks are completed in a discrete instance of time. Thus in the timing task, activity might accumulate tonically over the duration of the trial, whereas in the control task activity is generated phasically. Therefore if a temporal judgment is being compared with a discrete magnitude judgment, increased activation might be due to other factors such as sustained attention or time on task. *2*) The subtraction might also be eliminating parts of a network important for timing. For example, A Theory of Magnitude (ATOM) proposes that right inferior parietal lobe instantiates a shared magnitude estimator (Walsh 2003) rather than unique spatial or temporal networks. On such an account, contrasting temporal tasks to spatial tasks might subtract the very parts of the network critical, albeit not unique, to temporal judgment. The current experiment is concerned with neural networks involved with temporal dynamics of stimuli and is not designed to differentiate timing networks from other, potentially overlapping, magnitude processing systems.

Address for reprint requests and other correspondence: E. Wencil, c/o A. Chatterjee, 3 West Gates, 3400 Spruce St. Philadelphia PA 19104 (E-mail: ewencil@psych.upenn.edu).

Previous fMRI studies of interval timing have been motivated by variations of an information processing "internal clock." However, their designs and conclusions are not often tied to the components of these models. As originally proposed by Gibbon (1977), this class of models proposes three components in perceiving interval timing durations: an accumulating clock component that produces the timing signal, a memory component where the output of the accumulator is stored, and a comparator component where decision processing occurs (Fig. 1). A switch or gate is proposed to signal the accumulator that a task-relevant event is beginning and ending (Buhusi and Meck 2006). Attention is one mechanism hypothesized to influence the switch's functioning (Meck 1984; Meck and Benson 2002; Penney et al. 2000). Internal clock models have been successful in accounting for much of the psychophysical data relating to interval timing. Unfortunately, functional imaging studies have not consistently dissected these components. Therefore little is known about the neuroanatomical structures underlying these component processes.

The current study builds on earlier work in several important ways. First our paradigm used parametric fMRI to obviate the need to contrast temporal discrimination with another magnitude judgment (such as a spatial discrimination task). Specifically, we parametrically varied the stimulus durations to be compared. Importantly, the durations being compared were selected through pilot testing to be orthogonal to the difficulty in making comparisons of duration pairs. By ensuring that duration is orthogonal to the difficulty of making a comparison, the design allows us to tie activation patterns to independent components of the information processing model used for interval timing. We can infer that activations associated with the duration being timed are tied to clock/accumulator component, activations associated with levels of performance (i.e., % correct) are tied to comparator/decision making components, and activations associated to the presentation of duration to be timed are tied to attention. In addition, this design addresses two confounds described above. First, the parametric design obviates difficulties in interpretation resulting from the fact that judgments about time occur over time, and second, this design obviates the need for a control task that might subtract out regions of interest that might be part of a shared magnitude system (Walsh 2003).

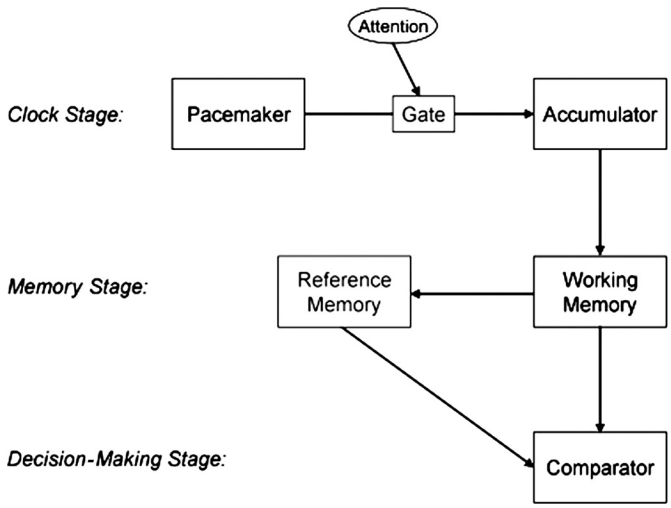

FIG. 1. An internal clock model of interval time perception. A graphical representation of the components of information processing that occurs while perceiving short durations. Pulses are counted by an accumulator. The output of the accumulator is transformed into a memory representation. The comparator judges the current memory trace against previously formed representations to make a temporal discrimination.

METHODS

Participants

Twelve paid subjects participated in this experiment (age: 23 ± 3 yr; 7 female). All participants were right handed, native English speakers without history of neurological or psychiatric symptoms. All participants provided written, informed consent in accordance with the policies of the University of Pennsylvania's Institutional Review Board.

Experimental design and procedure

Each subject performed a visual temporal discrimination task shown in Fig. 2. Each trial began with a centrally located red circle that oriented the subject to the task. After a 500 ms delay, the red circle was replaced by a green circle, labeled S1. S1 presentation varied between 300 and 1,500 ms in 300 ms intervals (i.e., 300, 600, 900, 1,200, or 1,500 ms). After S1, there was an interstimulus interval (ISI), represented by a red circle. The ISI spanned 4,000–5,200 ms to create jitter of the S2 presentation. This jittering allowed for separation of the evoked hemodynamic response of S1 and S2; in addition it prevented any rhythmic auditory features of the scan sequence from aiding subjects' performance on the temporal task. Following the ISI, the circle again appeared green, labeled S2. S2 remained on the screen for 300–1,500 ms in 300 ms intervals but was never the same duration as the S1. The trial concluded with a central fixation cross that served as an intertrial interval (ITI) ranging from 16.5 to 17.7 s. The subjects were instructed to attend to the duration of the S1 and S2 stimuli; after the S2 offset, the subject indicated whether S2 was longer or shorter than S1 via manual response with a MR-compatible button box. If S2 was longer, subjects responded with their right index finger; if S1 was shorter, subjects responded with their right middle finger.

The critical stimuli presented were the S1 and the S2 green circles. By design, the S1 duration and S2 duration were orthogonal to the difficulty of the judgment as indexed by response time and accuracy. Specifically, we ensured that the difficulty of each trial was not predicted by either the S1 duration or the S2 duration. We did this during a two-stage piloting process. We presented volunteers with the 20 possible S1/S2 combinations of the five durations (300, 600, 900, 1,200, and 1,500) when S1 and S2 are not the same. From their performance, we selected 14 S1/S2 comparison pairs (e.g., S1 = 300 ms and S2 = 600 ms or S1 = 300 ms and S2 = 1,500 ms) where the subset of S1s and S2s did not correlate with response time or accuracy. In this example, performance on the 300/600 pair would be slower and less accurate than on the 300/1,500 pair; this example importantly evidences that a 300 ms S1 does not provide information about the difficulty of the trial. The stimulus pairs (presented in Table 2) also met the following criteria: they included all of the durations and the correct response was counterbalanced across trials (½ of trials types had S2 being longer than S1; ½ of the trials types had S2 being shorter). In piloting phase 2, we verified that the resulting subset of S1 and S2 stimuli, that would be presented during imaging, remained orthogonal to performance. During imaging, each of the chosen discrimination pairs was presented 15 times, resulting in 210 duration discrimination trials across the scan session. Trials were randomized and presented to subjects in a sparse event-related fashion across 15 functional scans that lasted 5 min 35 s each. Response ("longer" or "shorter") and response times (RT) were collected during fMRI acquisition.

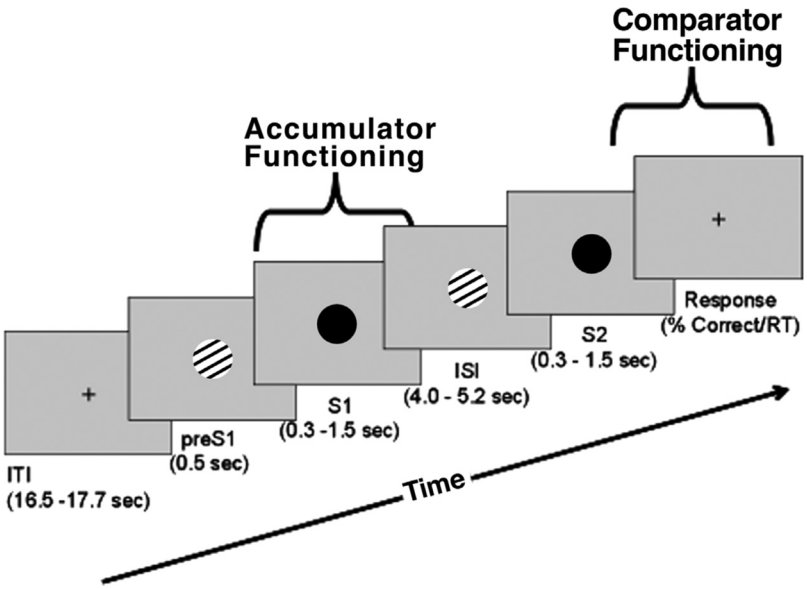

FIG. 2. Experimental design. Circles with horizontal lines appeared red during testing and black filled circles appeared green during testing. Participants performed a temporal discrimination task. Each trial began with a centrally presented fixation cross followed by the presentation of a red circle. After 500 ms, the circle changed from red to green (S1). Participants were instructed to attend to the duration of the green circle. After 300–1,500 ms, the circle became red for a variable duration ISI. Again the circle turned green (S2) for another 300–1,500 ms. Participants reported whether the second green circle was longer or shorter than the first green circle.

Data acquisition and analysis

T2*-weighted echo-planar, blood oxygenation level dependent (BOLD) images (T_R = 3 s, T_E = 30 ms, matrix size = 64 × 64, voxel size 3 × 3 × 3 mm) were acquired on a 3T Siemens TRIO scanner using a standard Siemens/MRI Devices eight-channel head coil. During each of the 15 functional scans 113 volumes were collected. The first six images were discarded to allow for steady-state magnetization. Forty-four 3-mm axial slices were acquired per volume. Head motion was minimized by placement of foam padding; furthermore on-line three-dimensional (3-D) prospective motion correction (PACE) was performed. High resolution, T1-weighted 3-D magnetization prepared rapid gradient echo (MPRAGE) images (T_R = 1620 ms, T_E = 3 ms, T_I = 950 ms, matrix size = 192 × 256, voxel size: 0.9766 × 0.9766 × 0.9766 mm) were also acquired for anatomical localization.

Stimulus presentation and response recording was controlled by E-prime (Psychology Software Tools) running on a computer located outside the scanner room. Stimuli were projected to a rear projection screen situated at the back of the scanner bore. Subjects viewed the projected image through a mirror mounted on the head coil. Responses were transmitted by a fiber-optic response pad system (fORP, Current Designs).

Data processing and analysis was conducted using Voxbo image-analysis software (www.voxbo.org). Prior to statistical analysis, we performed sinc-interpolation in time to correct for the order of slice acquisition, used a motion-correction algorithm to realign volumes to the first image acquired, and performed thresholding. The anatomical images were then normalized to a standard Montreal Neurological Institute (MNI) template, and the functional data were registered to the normalized anatomical data. Functional data were also spatially smoothed using a Gaussian kernel with a full width at half-maximum of 3 mm.

For each subject, the average power spectrum across voxels and across voxels and across scans was obtained, and the power spectrum fit with a 1/frequency function (Zarahn et al. 1997). This model of intrinsic noise was used during regression analyses with the modified general linear model (GLM) (Worsley and Friston 1995) to inform the estimates of intrinsic temporal autocorrelation. Temporal frequencies below that of the task were filtered from the data and represented in the intrinsic model of autocorrelation. Covariates modeled the following task conditions: the mean effect of S1 onset, modulation of the response by S1 duration, the mean effect of S2 onset, modulation of response by S2 duration and mean accuracy (% correct). S1 duration was orthogonalized to the mean effect S1 onset, as was S2 duration and mean accuracy to S2 onset. In addition, task covariates were mean normalized to retain orthogonality with the other task covariates. All task covariates were modeled as scaled delta functions convolved with a standard hemodynamic response function.

Random-effects analyses were performed for anatomically defined region of interests (ROIs). The regions, chosen a priori based on a review of the relevant literature, included: subregions of the basal ganglia (caudate, putamen, and globus pallidus), inferior frontal gyri (IFG) (BA 44), IFG (BA 45/46), IFG (BA 47/11), supplemental motor area (SMA), inferior parietal lobule (IPL), superior parietal lobule

TABLE 1. *Covariates used in modeling fMRI data*

Covariate Models		Covariate Relates to Internal Clock
S1 onset	Mean effect of S1 stimulus onset	Temporal attention: nonspecific effects of orienting to the stimulus and attending to time independent of the duration during which a putative accumulator operates.
S1 duration	Mean centered effect of the S1 stimulus duration	Accumulator: neural response that is linearly related to the duration of the S1 stimulus, therefore accumulation variability uniquely explained by the duration being timed.
S2 onset	Mean effect of S2 stimulus onset	Nuisance variable: nonspecific effects of orienting which are unable to be dissociated from ITI related neural activity.
S2 duration	Mean centered effect of the S2 stimulus duration	Nuisance variable: undifferentiated neural response related to accumulation, comparison, decision uncertainty and motor preparation.
Difficulty	Mean accuracy across subjects for each timing trial	Comparator: neural response where intensity neural activity is related to the difficulty of the comparison.

Covariates used in modeling our fMRI data, and our interpretations of the activation patterns related to the covariates of interest. By design, the three covariates of interest, S1, S1 duration, and difficulty, were orthogonal to each other.

TABLE 2. *List of S1–S2 comparison pairs*

S1 Duration, ms	*S2 Duration, ms*	*Accuracy*
300	600	0.941
300	900	0.936
600	300	0.937
600	900	0.874
600	1200	0.953
900	300	0.937
900	600	0.840
900	1200	0.915
900	1500	0.963
1200	300	0.990
1200	900	0.604
1200	1500	0.895
1500	300	0.974
1500	600	0.905

Average accuracy across the 12 subjects on the 14 trial types presented. These values were modeled as the accuracy covariate for the imaging data.

(SPL), and superior temporal gyrus. We did not include a cerebellar ROI as we lacked consistent signal in this region. Masks were drawn by graduate and medical student trainees and then reviewed by a senior neurologist. Time series within each subject was averaged across all voxels for each anatomically defined ROI. Then a normalized beta value for each covariate of interest (S1 onset, S1 duration and mean accuracy) was calculated from each subject's GLM. Loading of the two nuisance covariates, mean effect of S2 onset and modulation of response by S2 duration, were not of interest because they are ambiguously related to components of the internal clock (see Table 1). Effect sizes of the covariates of interest were tested groupwise in independent one-sample *t*-test using SPSS v. 14 (SPSS).

RESULTS

Behavioral results

Overall, subjects performed the visual temporal discrimination task well (accuracy = 90 ± 6.4%, RT = 831.9 ± 130.3 ms). As expected, performance improved as the difference between the two durations being compared increased (see Fig. 3). Accuracy served as our index of task difficulty in imaging analysis. Accuracy is preferable to RT for this design as participants were instructed to wait until the end of the S2 duration before responding. During trials where S2 was longer than S1, subjects could prepare their response in advance. Therefore response time is not a meaningful measure of the difficulty of the task as evidenced by the dramatic decrease in reaction time during the +300 and +600 ms conditions illustrated in Fig. 3*B*. By contrast, accuracy reflects the difficulty in making comparisons of temporal durations.

Consistent with our pilot data, S1 duration was orthogonal to the difficulty of comparing duration pairs in each trial. None of the correlations were significant (S1 and accuracy, $r = -0.30$, $P = 0.62$; S1 and RT, $r = -0.06$, $P = 0.93$). Therefore activation patterns associated with each of the parametric covariates are independently generated.

Activations associated with S1 onset

We modeled the mean effect of S1 stimulus onset. Examination of this covariate informs as to nonspecific effects of orienting to the stimulus and attending to time independent of the duration during which a putative accumulator operates. ROI analysis revealed several regions that had a significant increase in BOLD response when subjects' attention was cued toward the temporal qualities of the visual stimulus. Significant responses were seen in inferior frontal regions including the right pars triangularis extending dorsally into BA 46 as well as bilateral pars opercularis of the inferior frontal gyri. Left superior angular and posterior supramarginal gyri of the inferior parietal cortex and the caudate also show significant activations to the onset of S1.

Activations correlated with S1 duration

A separate covariate modeled the duration of presentation of the S1 stimulus. Significant loading on this covariate indicates the presence of a neural response that is linearly related to the duration of stimulus. Although the S1 onset covariate might have some unspecific accumulation in common with the S1 duration covariate, the orthogonal S1 duration covariate is designed to express variability uniquely explained by the temporal duration of the signal. Several regions with significant responses to duration were identified: left inferior frontal regions including pars triangularis and lateral orbital gyrus as well as the superior temporal gyrus and SMA (Table 3). Interestingly, the homologous regions on the right were not activated (Fig. 4*A*). We performed ad hoc analyses on the four significant ROIs to plot the relationship between duration and evoked response (Fig. 5). Each ROI showed a monotonic relationship when beta values for each subject were plotted against each S1 duration (SMA: $r = 0.74$ $P = 0.014$; IFG

TABLE 3. *fMRI region of interest results*

	S1 Onset		S1 Duration		Accuracy	
	Left	Right	Left	Right	Left	Right
Basal ganglia: caudate	**1.41 ± 0.57**	0.70 ± 0.57	−0.07 ± 0.31	−0.06 ± 0.35	−0.03 ± 0.33	0.04 ± 0.38
Basal ganglia: putamen	−0.25 ± 0.53	−0.58 ± 0.56	0.46 ± 0.33	−0.18 ± 0.29	−0.08 ± 0.31	0.03 ± 0.28
Basal ganglia: globus pallidus	−0.83 ± 0.59	−0.94 ± 0.63	0.11 ± 0.32	−0.35 ± 0.29	−0.04 ± 0.21	−0.04 ± 0.30
IFG (BA 44)	**1.92 ± 0.82**	**2.55 ± 0.93**	0.38 ± 0.28	0.25 ± 0.31	0.11 ± 0.24	**0.43 ± 0.25**
IFG (BA 45/46)	1.14 ± 0.70	**1.76 ± 0.54**	**0.54 ± 0.30**	**0.24 ± 0.30**	**0.44 ± 0.26**	0.15 ± 0.26
IFG (BA 47/11)	−1.30 ± 0.79	−1.47 ± 0.69	**0.58 ± 0.32**	0.01 ± 0.32	−0.39 ± 0.34	−0.17 ± 0.41
SMA	1.04 ± 0.63	0.10 ± 0.71	**0.75 ± 0.39**	0.62 ± 0.37	0.15 ± 0.34	0.41 ± 0.30
IPL	1.61 ± 0.83	0.96 ± 0.61	0.07 ± 0.31	0.07 ± 0.27	0.25 ± 0.26	−0.06 ± 0.32
SPL	0.32 ± 0.97	0.51 ± 1.04	−0.04 ± 0.26	−0.37 ± 0.24	0.00 ± 0.26	−0.32 ± 0.28
Superior temporal	0.64 ± 0.70	1.20 ± 0.80	**0.61 ± 0.33**	0.17 ± 0.31	0.03 ± 0.27	−0.02 ± 0.30

Bolded *t*-values are significant at $P < 0.05$. IFG, inferior frontal gyrus; SMA, supplementary motor area; IPL, inferior parietal lobule; SPL, superior parietal lobule.

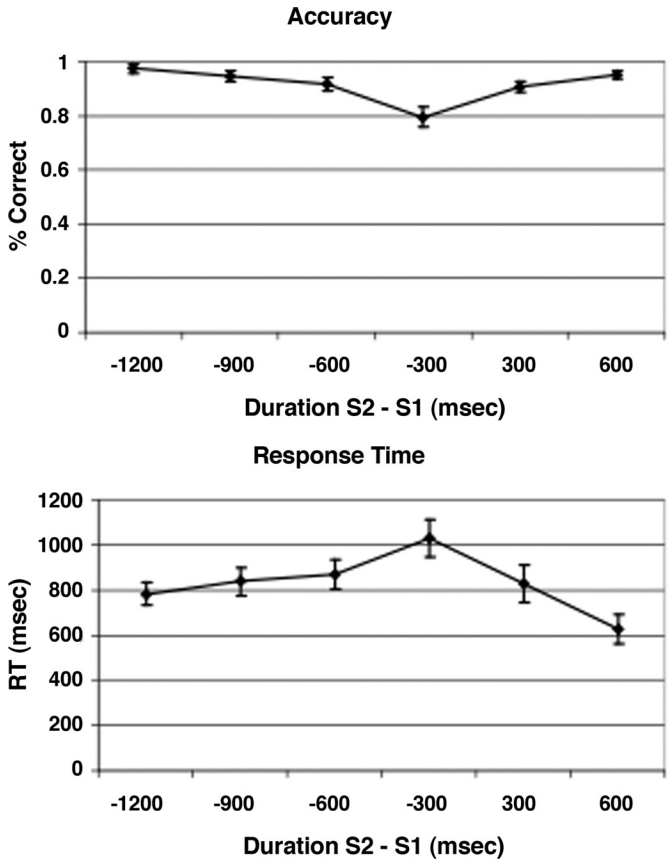

FIG. 3. Behavioral results. Mean accuracy and response times (SE) plotted by the duration of S2 minus the duration of S1. For example, S2 (the second green circle) lasting 600 ms and S1 (the first green circle) lasting 1,200 ms would be included in the −600 bin. The 14 trial types averaged here are presented individually in Table 2.

45/46: $r = 0.56$ $P = 0.152$: IFG 47/11: $r = 0.85$ $P = 0.04$, superior temporal: $r = 0.70$ $P = 0.04$).

Activations correlated with accuracy

By design, our study allows us to test for independent responses to the duration of stimulus presentation and the difficulty of timing assessment. A covariate modeled neural response as a function of the mean accuracy across subjects for each timing trial, which we used as a measure of difficulty. The ROI analysis revealed two regions in which the BOLD response varied linearly with the difficulty of making a temporal decision, as measured by accuracy. Specifically, left inferior frontal regions including the left pars triangularis extending into BA 46 and the right frontal operculum activity correlated with difficulty. Importantly, although these activations partially overlap spatially with those found in response to S1 duration, these covariates were designed to be orthogonal and the activation patterns do not represent shared variance in the model. (Fig. 4*B*).

DISCUSSION

The ability to process and represent intervals of time is critical to most behavior. Models describing the components involved in processing temporal information usually invoke an accumulator and a comparator. These models are applied to the perception of durations from hundreds of milliseconds to seconds. However, little is known about how the components of this putative internal clock model map onto neural structures. We have identified neural regions that correspond to these components during short "automatic-timing" durations.

In the current study, subjects performed a temporal discrimination task during fMRI acquisition that allowed us to isolate discrete neural activity evoked by different components of a putative internal clock model. By design, stimuli durations were orthogonal to the difficulty in comparing duration pairs, thus allowing us to assess the variance in neural activity accounted for independently by these factors. We reasoned that neural activity that correlated with S1 duration would represent accumulator networks. We also reasoned that neural activity that correlated with the difficulty in making comparisons of duration pairs would represent comparator networks. The inferential strength of this study relies on the parametric design that allows us to isolate different components of the internal clock while eliminating the pitfall of contrasting timing judgments to other perceptual judgments (e.g., color hue) that happens at a distinct instance in time. Using parametric fMRI also frees the results from confounds that might follow from subtractions of the overlapping networks engaged in judging magnitudes.

As previously proposed, the accumulating clock stage creates a neural timing signal by the functioning of a pacemaker, switch/gate, and accumulator. The pacemaker is envisioned to produce an accumulating, regular, periodic pulse that reliably maps onto the passage of time. The accumulator collects the input from the pacemaker and supplies an output of this temporal code to the memory and comparator stages. Gibbon originally theorized that this was accomplished by counting the action potentials of the Poisson pacemaker and then summing the magnitude of these pulses linearly (Gibbon 1977). Others have argued for a similar architecture but have theorized the output is logarithmically related to the counted pulses (Treisman et al. 1990). Multiple oscillator models differ from the traditional pacemaker/accumulator architecture (Church and Broadbent 1990; Miall 1989). In these models, the accumulator tracks different phases of the oscillators; at the start of the interval, the oscillators begin in phase but as the interval progresses, they fall out of phase with each other. Therefore accumulator tracks the pattern of asynchrony of these oscillations rather than constantly monitoring the mounting number of "beats." These two models would lead to very different neural signals; unlike the multiple oscillator models, the traditional accumulator clock models' signal would increase with the passage of time. The activation patterns we observed in the left inferior frontal, SMA, and superior temporal are more consistent with accumulating pulses than with multiple oscillators. Thus these activation patterns provide evidence of a linear metric of time that is consistent with a pacemaker/accumulator model. The data are uninformative with respect to other models such as those invoking beat frequencies or memory decay.

Several neural regions, including the basal ganglia, posterior parietal cortex, frontal cortex, and cerebellum, have been associated with the accumulator clock stage; however, their precise role remains unclear. Pharmacological manipulations of dopamine have implicated striatal involvement in the clock component (Drew et al. 2003; Lewis and Miall 2006b; Mac-

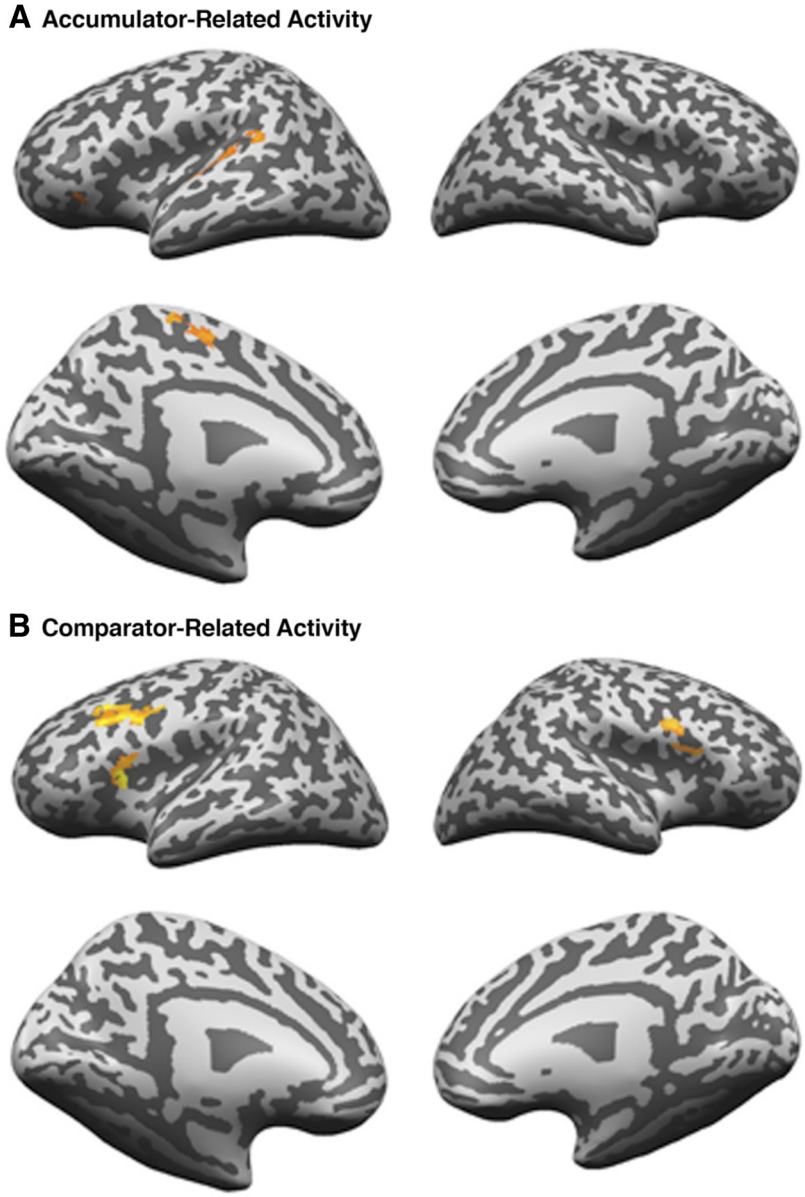

FIG. 4. fMRI results. *A*: signal trends within regions of interest (ROIs) that varied with S1 duration showing left pars triangularis and left lateral orbital gyrus of the inferior frontal gyrus as well as left superior temporal gyrus and supplemental motor area. *B*: signal trends within ROIs that varied with accuracy showing left pars triangularis and right frontal operculum activity.

Donald and Meck 2004, 2005; Maricq and Church 1983; Meck 1986, 1996; Rakitin et al. 2006). Neurons in task related sensory regions such as the posterior parietal cortex during spatial tasks and V4 during a visual orientation task have also been demonstrated to represent the passage of short intervals of time (Leon and Shadlen 2003). Whereas TMS of V5 disrupts visual timing, TMS over posterior parietal cortex disrupts both visual and auditory timing, suggesting the parietal cortex is involved in a more generalized clock mechanism (Bueti et al. 2008). Previous imaging studies attempting to isolate neural regions associated with clock mechanisms confirmed involvement of the basal ganglia and posterior parietal cortex; in addition, these studies revealed frontal activity relating to the accumulating clock stage (Harrington et al. 2004; Jech 2005; Onoe et al. 2001; Rao et al. 2001). Specifically, bilateral activity in the monkey dorsolateral prefrontal cortex, posterior inferior parietal cortex, basal ganglia, and posterior cingulate correlated with the duration of the target being perceived during a time discrimination task (Onoe et al. 2001). In the first fMRI study attempting to dissociate components of timing, bilateral caudate, right putamen, right inferior parietal cortex, and bilateral premotor cortex were activated early (within 5 s of the onset of the discrimination task); the authors argued that these regions were involved in encoding duration (Rao et al. 2001). In a recent study that elegantly addressed the issue surrounding sustained attention, SMA was activated during both the target and the probe durations; the authors reason that SMA is thus involved with the clock mechanism (Coull et al. 2008). In addition to these regions, the left cerebellum was implicated in the encoding of durations in the second imaging study (Harrington et al. 2004). Although it remains controversial, the lateral cerebellum has also been implicated through lesion and imaging studies as serving the clock mechanisms (Ivry 1996; Ivry et al. 2002).

In the current study, we found that activity in a subset of these regions, including left IFG (BA 45/46), superior temporal, and SMA, had significant loading on the covariate modeling S1 duration. We conclude that the linearly related activity

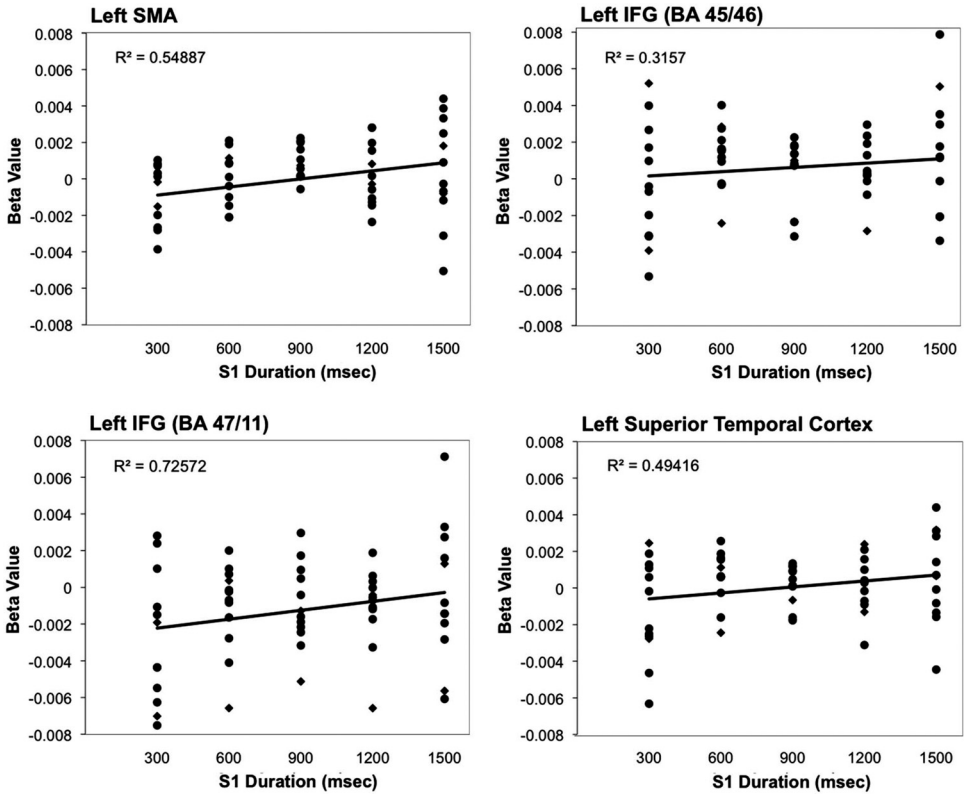

FIG. 5. fMRI results. Ad hoc analyses performed to verify a monotonic relationship of S1 duration and evoked response within each significant ROI. The average beta value of the voxels with each ROI for each subject is plotted against the S1 duration.

of these regions reflects accumulator functioning. Because the duration being timed is orthogonal to the onset and difficulty of that trial, we can confidently infer that these activations are independent of temporal attention (conceived generally) or comparator and decision making functions. Operationalizing accumulator-related networks as regions that increase linearly with the duration being timed does not rule out that sustained attention is driving these effects; however, sustained attention might be the material that the timing signal is created from. Given the temporal constraints of fMRI, we do not attempt to disambiguate sub-components of the pacemaker/accumulator stage. One mechanism by which sustained attention might explain our effects is by directing the switch to remain closed allowing the accumulator to count beats. Therefore it remains unknown whether these activations relate to the increased time spent attending or to time spent accumulating. However, our findings are consistent with previous claims (Ferrandez et al. 2003; Hinton and Meck 2004; Macar et al. 2004) that the left frontal triangularis and SMA encode temporal intervals within clock mechanisms. Two previous visual timing studies also report superior temporal activation but attribute this activation to auditory strategies (Coull et al. 2004; Ferrandez et al. 2003). Eight of our subjects reported using sub-auditory strategies such as internal humming to assist with the temporal discrimination task. The left superior temporal activation may reflect this strategy as opposed to a purely timing mechanism. Further studies are needed to determine the extent to which different modalities influence internal clock structures. All accumulator-related activations in our study were lateralized to the left hemisphere. This is inconsistent with reports of right lateralization of timing deficits in the patient literature (Harrington et al. 1998; Vidalaki et al. 1999). However, the effect sizes are often small and not all investigators have found significant asymmetries (Rubia et al. 1997). Our data suggest that accumulator/clock functioning is left lateralized, whereas other components involved in timing engage both hemispheres.

We have all experienced the subjective phenomenon of time racing by very quickly or conversely, the experience of time coming to a halt where seconds begin to feel like hours. Attention has been theorized to modulate the internal clock to explain this subjective lengthening and shortening of duration. In a seminal experiment, Coull and colleagues successfully varied subjects' attention to either temporal or color attributes of a stimulus during a discrimination task (Coull et al. 2004). Imaging during this paradigm showed timing-related parametric increases in activity throughout a corticostriatal network. Some have proposed that sharing attentional resources with other tasks alters attention's control of the switch in the clock mechanism (Macar et al. 1994). In other words, as less attention is directed to temporal qualities, the switch malfunctions and pulses are missed by the accumulator, thus time seems shorter.

In our design, the onset of S1 served as a cue to pay attention to temporal durations. Activity generated by the onset of S1 could represent a temporal alerting function, although our design remains agnostic about whether this cue to pay attention is in fact specific to time per se. We found onset of the S1 was associated with left caudate, left inferior parietal (superior angular and posterior supramarginal gyrus), right frontal triangularis (BA 45/46), and bilateral frontal opercula (BA 44). These activations could represent temporal attention or conversely, these activations (especially the left IPL) might represent a more general attentional control system. We cannot rule out that these activations are not evoked by other general cognitive demands such as nonspecific cuing and motor preparation. Our findings are similar to past imaging studies in that

caudate and posterior parietal regions are activated during interval timing tasks. However, as the basal ganglia and IPL activations did not correlate with S1 duration, we did not confirm that these regions serve as the neural substrate of the accumulator.

The output of the accumulator is theorized to be stored as a single value referred to as "reference memory." The form of this temporal representation remains unclear: some envision reference memory as a working memory buffer (Lewis and Miall 2006b), whereas others describe the transformed output as a stored long term memory trace (Hinton and Meck 1997; Meck 1988; Meck et al. 1984; Perbal et al. 2001). These two alternatives are not mutually exclusive; many tasks involving interval timing call on a need to hold these values in an active working memory buffer while at the same time reinforced traces can be stored for later recall and use. Within the current design, regions activated during the ISI would support temporal working memory—however, our design did not allow us to distinguish neural activity evoked during the ISI from that evoked from S1 presentation. The bilateral inferior frontal activation evoked by S1 presentation might relate to memory stores involved in interval timing, but further studies are needed to address this component of interval timing.

In everyday tasks in which discriminating a duration is necessary, the current duration is compared with a previous temporal duration. The comparator is theorized to make this decision of longer or shorter. Different theories propose different mechanisms including on-line ratio comparison (Gibbon 1977), comparison of the current on-line asynchrony of multiple oscillator phases (Church and Broadbent 1990), absolute discrepancy rules (Treisman et al. 1990), or assessment of the phase asynchrony at offset (Miall 1989), all compared with a stored temporal representation. Very little is known about the neural basis of the comparator. Dissociating neural activity relating to the comparator from that of the accumulating clock and memory stages has been difficult. Prior imaging studies that have attempted this dissociation found several areas including bilateral cerebellar, bilateral prefrontal, left middle-frontal, bilateral parietal, left superior temporal, thalamus, and SMA activity during the comparison and decision-making period of temporal discrimination tasks (Harrington et al. 2004; Livesey et al. 2007; Rao et al. 2001). The authors of a recent report that found that superior temporal cortex was activated during the S2 but not S1 of a duration discrimination task concluded that superior temporal cortex is involved in temporal decision-making (Coull et al. 2008). We found that neural activity in a subset of these regions increased with the difficulty of making a temporal comparison. We interpret significant loading on this covariate as indicating a comparator operation in which the intensity or duration of neural activity is related to the difficulty of the comparison. Specifically, activity within the left frontal triangularis (BA 45/46) and right frontal operculum (BA 44) was consistent with these regions serving as a comparator network. Alternatively, decision uncertainty independent of comparator operations might account for these effects. However, it is unknown if the theoretical distinction of decision uncertainty and operation of a comparator is neurally realized.

In summary, our data demonstrate that distributed neural networks subserve interval timing. To think that one or the other hemisphere dominates in representing time would be a mistake. Attending to time engages the left posterior parietal, striatal, and bilateral inferior frontal regions. Accumulator components of interval timing appear to be lateralized to the left hemisphere in right handed individuals, specifically engaging left inferior frontal, superior temporal, and the SMA regions. The comparator component of timing judgments involves the inferior frontal cortices bilaterally. These data suggest that interval timing abilities arise from the convergence of independent activations of overlapping neural systems.

ACKNOWLEDGMENTS

The authors acknowledge P. Widick for assistance with fMRI analyses and B. Bromberger for help preparing figures.

GRANTS

This work was supported by the National Institutes of Health Grants DC-0487 to A. Chatterjee and MH-76227 to H. B. Coslett.

DISCLOSURES

No conflicts of interest are declared by the authors.

REFERENCES

Brunia CH, de Jong BM, van den Berg-Lenssen MM, Paans AM. Visual feedback about time estimation is related to a right hemisphere activation measured by PET. *Exp Brain Res* 130: 328–337, 2000.

Bueti D, Bahrami B, Walsh V. Sensory and association cortex in time perception. *J Cogn Neurosci* 20: 1054–1062, 2008.

Buhusi CV, Meck WH. Time sharing in rats: a peak-interval procedure with gaps and distracters. *Behav Process* 71: 107–115, 2006.

Casini L, Macar F. Prefrontal slow potentials in temporal compared to nontemporal tasks. *J Psychophysiol* 10: 225–264, 1996.

Church RM, Broadbent HA. Alternative representations of time, number, and rate. *Cognition* 37: 55–81, 1990.

Coull J, Nobre A. Dissociating explicit timing from temporal expectation with fMRI. *Curr Opin Neurobiol* 18: 137–144, 2008.

Coull JT, Vidal F, Nazarian B, Macar F. Functional anatomy of the attentional modulation of time estimation. *Science* 303: 1506–1508, 2004.

Drew MR, Fairhurst S, Malapani C, Horvitz JC, Balsam PD. Effects of dopamine antagonists on the timing of two intervals. *Pharmacol Biochem Behav* 75: 9–15, 2003.

Ferrandez AM, Hugueville L, Lehericy S, Poline JB, Marsault C, Pouthas V. Basal ganglia and supplementary motor area subtend duration perception: an fMRI study. *Neuroimage* 19: 1532–1544, 2003.

Gibbon J. Scalar expectancy theory and Weber's Law in animal timing. *Psychol Rev* 84: 279–325, 1977.

Harrington DL, Boyd LA, Mayer AR, Sheltraw DM, Lee RR, Huang M, Rao SM. Neural representation of interval encoding and decision making. *Brain Res Cogn Brain Res* 21: 193–205, 2004.

Harrington DL, Haaland KY. Neural underpinnings of temporal processing: a review of focal lesion, pharmacological, and functional imaging research. *Rev Neurosci* 10: 91–116, 1999.

Harrington DL, Haaland KY, Knight RT. Cortical networks underlying mechanisms of time perception. *J Neurosci* 18: 1085–1095, 1998.

Hinton SC, Meck WH. The "internal clocks" of circadian and interval timing. *Endeavour* 21: 82–87, 1997.

Hinton SC, Meck WH. Frontal-striatal circuitry activated by human peak-interval timing in the supra-seconds range. *Brain Res Cogn Brain Res* 21: 171–182, 2004.

Ivry RB. The representation of temporal information in perception and motor control. *Curr Opin Neurobiol* 6: 851–857, 1996.

Ivry RB, Spencer RM, Zelaznik HN, Diedrichsen J. The cerebellum and event timing. *Ann NY Acad Sci* 978: 302–317, 2002.

Jech RC Wackermann J, Vymazal J. Cumulative blood oxygenation-level-dependent signal changes support the "time accumulator" hypothesis. *Neuroreport* 16: 1467–1471, 2005.

Kawashima R, Okuda J, Umetsu A, Sugiura M, Inoue K, Suzuki K, Tabuchi M, Tsukiura T, Narayan SL, Nagasaka T, Yanagawa I, Fujii T, Takahashi S, Fukuda H, Yamadori A. Human cerebellum plays an important role in memory-timed finger movement: an fMRI study. *J Neurophysiol* 83: 1079–1087, 2000.

Lang W, Obrig H, Lindinger G, Cheyne D, Deecke L. Supplementary motor area activation while tapping bimanually different rhythms in musicians. *Exp Brain Res* 79: 504–514, 1990.

Lejeune H, Maquet P, Bonnet M, Casini L, Ferrara A, Macar F, Pouthas V, Timsit-Berthier M, Vidal F. The basic pattern of activation in motor and sensory temporal tasks: positron emission tomography data. *Neurosci Lett* 235: 21–24, 1997.

Leon MI, Shadlen MN. Representation of time by neurons in the posterior parietal cortex of the macaque. *Neuron* 38: 317–327, 2003.

Lewis PA, Miall RC. Distinct systems for automatic and cognitively controlled time measurement: evidence from neuroimaging. *Curr Opin Neurobiol* 13: 250–255, 2003.

Lewis PA, Miall RC. A right hemispheric prefrontal system for cognitive time measurement. *Behav Processes* 71: 226–234, 2006a.

Lewis PA, Miall RC. Remembering the time: a continuous clock. *Trends Cogn Sci* 10: 401–406, 2006b.

Livesey AC, Wall MB, Smith AT. Time perception: manipulation of task difficulty dissociates clock functions from other cognitive demands. *Neuropsychologia* 45: 321–331, 2007.

Macar F, Anton JL, Bonnet M, Vidal F. Timing functions of the supplementary motor area: an event-related fMRI study. *Brain Res Cogn Brain Res* 21: 206–215, 2004.

Macar F, Grondin S, Casini L. Controlled attention sharing influences time estimation. *Mem Cogn* 22: 673–686, 1994.

Macar F, Lejeune H, Bonnet M, Ferrara A, Pouthas V, Vidal F, Maquet P. Activation of the supplementary motor area and of attentional networks during temporal processing. *Exp Brain Res* 142: 475–485, 2002.

Macar F, Vidal F, Casini L. The supplementary motor area in motor and sensory timing: evidence from slow brain potential changes. *Exp Brain Res* 125: 271–280, 1999.

MacDonald CJ, Meck WH. Systems-level integration of interval timing and reaction time. *Neurosci Biobehav Rev* 28: 747–769, 2004.

MacDonald CJ, Meck WH. Differential effects of clozapine and haloperidol on interval timing in the supraseconds range. *Psychopharmacology* 182: 232–244, 2005.

Maricq AV, Church RM. The differential effects of haloperidol and methamphetamine on time estimation in the rat. *Psychopharmacology* 79: 10–15, 1983.

Meck WH. Attentional bias between modalities: effect on the internal clock, memory, and decision stages used in animal time discrimination. *Ann NY Acad Sci* 423: 528–541, 1984.

Meck WH. Affinity for the dopamine D2 receptor predicts neuroleptic potency in decreasing the speed of an internal clock. *Pharmacol Biochem Behav* 25: 1185–1189, 1986.

Meck WH. Hippocampal function is required for feedback control of an internal clock's criterion. *Behav Neurosci* 102: 54–60, 1988.

Meck WH. Neuropharmacology of timing and time perception. *Brain Res Cogn Brain Res* 3: 227–242, 1996.

Meck WH, Benson AM. Dissecting the brain's internal clock: how frontal-striatal circuitry keeps time and shifts attention. *Brain Cogn* 48: 195–211, 2002.

Meck WH, Church RM, Olton DS. Hippocampus, time, and memory. *Behav Neurosci* 98: 3–22, 1984.

Meck WH, Malapani C. Neuroimaging of interval timing. *Cogn Brain Res* 21: 133–137, 2004.

Meck WH, Penney TB, Pouthas V. Cortico-striatal represenation of time in animals and humans. *Curr Opin Neurobiol* 18: 1–8, 2008.

Miall RC. The storage of time intervals using oscillating neurons. *Neural Comput* 1: 359–371, 1989.

Onoe H, Komori M, Onoe K, Takechi H, Tsukada H, Watanabe Y. Cortical networks recruited for time perception: a monkey positron emission tomography (PET) study. *Neuroimage* 13: 37–45, 2001.

Penney TB, Gibbon J, Meck WH. Differential effects of auditory and visual signals on clock speed and temporal memory. *J Exp Psychol Hum Percept Perform* 26: 1770–1787, 2000.

Perbal S, Ehrle N, Samson S, Baulac M, Pouthas V. Time estimation in patients with right or left medial-temporal lobe resection. *Neuroreport* 12: 939–942, 2001.

Pouthas V, Garnero L, Ferrandez AM, Renault B. ERPs and PET analysis of time perception: spatial and temporal brain mapping during visual discrimination tasks. *Hum Brain Mapp* 10: 49–60, 2000.

Rakitin BC, Scarmeas N, Li T, Malapani C, Stern Y. Single-dose Levodopa administration and aging independently disrupt time production. *J Cogn Neurosci* 18: 376–387, 2006.

Rao SM, Harrington DL, Haaland KY, Bobholz JA, Cox RW, Binder JR. Distributed neural systems underlying the timing of movements. *J Neurosci* 17: 5528–5535, 1997.

Rao SM, Mayer AR, Harrington DL. The evolution of brain activation during temporal processing. *Nat Neurosci* 4: 317–323, 2001.

Rubia K, Overmeyer S, Taylor E, Brammer M, Williams S, Simmons A, Andrew C, Bullmore E. Prefrontal involvement in "temporal bridging" and timing movement. *Neuropsychologia* 36: 1283–1293, 1998.

Rubia K, Schuri U, von Cramon DY, Poeppel E. Time estimation as a neuronal network property: a lesion study. *Neuroreport* 8: 1273–1276, 1997.

Tracy JI, Faro SH, Mohamed FB, Pinsk M, Pinus A. Functional localization of a "time keeper" function separate from attentional resources and task strategy. *Neuroimage* 11: 228–242, 2000.

Treisman M, Faulkner A, Naish PL, Brogan D. The internal clock: evidence for a temporal oscillator underlying time perception with some estimates of its characteristic frequency. *Perception* 19: 705–743, 1990.

Vidalaki VN, Ho MY, Bradshaw CM, Szabadi E. Interval timing performance in temporal lobe epilepsy: differences between patients with left and right hemisphere foci. *Neuropsychologia* 37: 1061–1070, 1999.

Walsh V. A theory of magnitude: common cortical metrics of time, space and quantity. *Trends Cogn Sci* 7: 483–488, 2003.

Worsley KJ, Friston KJ. Analysis of fMRI time-series revisited - again. *Neuroimage* 2: 173–182, 1995.

Zarahn E, Aguirre GK, D'Esposito M. Empirical analyses of BOLD fMRI statistics. II. Spatially smoothed data collected under null-hypothesis conditions. *Neuroimage* 1997: 199–212, 1997.